THE CREEP OF MATERIAL OBTAINED USING SLS TECHNOLOGY

JERZY BOCHNIA, SLAWOMIR BLASIAK

Kielce University of Technology, Faculty of Mechatronics and Mechanical Engineering, Department of Mechanical Technology and Metrology, Kielce, Poland

DOI : 10.17973/MMSJ.2020_03_2019022

e-mail: jbochnia@tu.kielce.pl

This paper discusses the results of the creep of material obtained with the use of the SLS additive technology. The author described the creep test, and a selected rheological model was adjusted to the creeping curve obtained in an experiment way. The parameter values of the rheological model were estimated. The anisotropy of the rheological properties of the material with regard to the print direction was determined.

KEYWORDS

Additive Technologies, Creep of Material, Rheological Model

1 INTRODUCTION

The main advantage of the Selective Laser Sintering technology (SLS) is the fact that the manufactured elements after cooling down to the ambient temperature are suitable for use. Applying this method on an industrial scale determines scientific research regarding the mechanical and rheological properties of those materials. This way of building materials and at the same time, creating a material which the model is built from leads to the anisotropy of the mechanical properties. This problem was described in a number of papers, e.g. [Bass 2016] [Adamczak 2017]. With no doubt it is a disadvantage of this technology in relation to e.g. plastic injection molding or mechanical processing [Nowakowski 2017] where the problems of anisotropy are not found or are of lesser significance. The extensive characteristics of the additive technologies (including SLS), the theoretical foundations of those technologies, proper equipment and materials as well as the results of some research might be found in the paper of [Gibson 2010]. Example papers regarding testing powders applied for laser sintering include [Verbelen 2017] [Vasquez 2014] [Kozior 2019]. This paper presents the results of the creep test conducted with the SLS technology using the printer - Formiga P100. The author described how the samples were made and the creep test was conducted as well as the selected rheological model [Schmidt 2017] was adjusted to the creep curve obtained in an experimental way. The parameter values of the rheological model were estimated. The test results might be helpful in various kinds of modelling of engineering calculations [Takosoglu 2014] and construction works [Blasiak 2014] or research papers [Blasiak 2016].

2 METHODS

The samples for the creep test were made of PA 2200 polyamide powder laser-sintered with the use of the Formiga P100 manufactured by EOS. The layer thickness of 0.1 mm and the laser power of 21 W were applied. The diameter of the focused laser beam was approximately 0.42 mm. Cylindrical samples of the following nominal dimensions: D = 15 mm and H = 15 mm were used for the tests. The solid models of samples were drawn in CAD 3D software and saved in a digital file with *.stl extension using the triangulation parameters in export options: resolution – adjusted, deviation – the tolerance of 0.016 mm, angle – the tolerance of 50. Subsequently, with the use of Magic software, the triangulation was checked and the verified *.stl files were imported to Rp Tools software, and then to *.sli file. An example of arranging the samples on the build tray of the printing machine was presented in Figure 1.

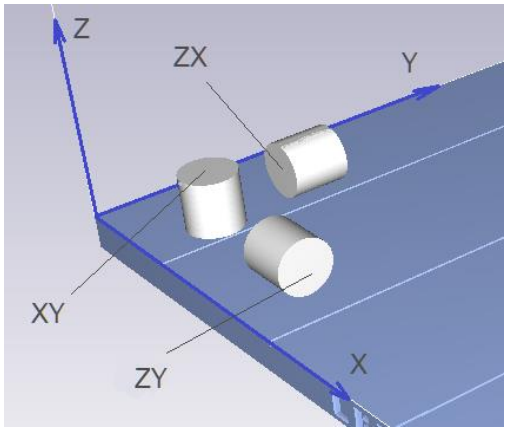

Figure 1. Sample arrangement on the build tray of the printing machine

The creep test was made using the Ispect mini (Hegewald & Peschke MPT GmbH) testing machine with range of 3 kN. Measurement, data acquisition and setting the parameters of the test were performed in the LABMASTER program (Version 2.5.3.21), which is supplied with the Inspect mini machine. In order to grip the cylindrical samples, flat plates were applied (the lower tilting plate was used) The samples were individually vertically placed in the central position of the lower plate, and subsequently, the upper plate attached in the machine handle was pushed back against it so that it could contact the flat surface of the sample. The preload should not exceed 10 N. Then, all indications, i.e. load, distance, time were tarnished (zeroed) and the test was restarted. Figure 2 shows an example sample placed between two plates.

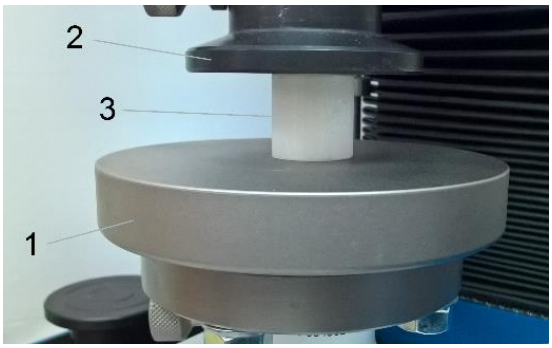

Figure 2. The sample prepared for the creep test. 1 – lower tilting plate, 2 – upper plate, 3 – sample

In the first block of the program, the force value of 1,400 N was applied, which was an equivalent to the tension of 7,926 MPa at the displacement velocity of the gripping plate v = 0.5 mm/s. The second block of the program consisted in bringing the plate to a stop and maintaining its constant value at the level of 1,400 N (tension 7,926 MPa) for 18,000 seconds. During this time, a slight increase in deformation was detected – the creep of the material recorded as a graph. The third block of the program includes bringing the plate to its initial (zero) position.

At that time, the weights were removed from the sample. An example graph of the entire creep test was presented in Figure 3.

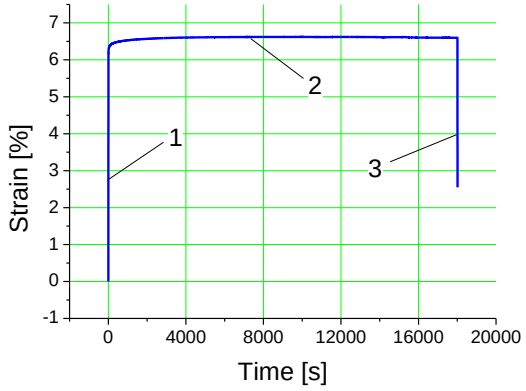

Figure 3. An example graph of the creep test, material PA 2200. 1 – strain which is a result of a quasi-unit stress leap, 2 – creep curve, 3 – offload.

The mathematical description of the creeping curve (2) with the use of an ideal body model so that this description is of physical importance is a crucial problem. The Kelvin-Voight model of the second order or otherwise the five-parameter Kelvin-Voight model with the spring E_0 and two basic Kelvin elements, where E_1 and E_2 represent the elastic modulus, while μ_1 and μ_2 are the viscosity characterizing the damper in the Kelvin elements. This model was presented in Figure 4.

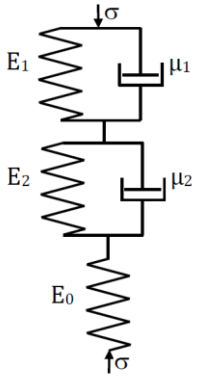

Figure 4. The Kelvin–Voight model applied to describe the creep of the studied samples.

In the case of the creep when $\sigma = \sigma_0$, i.e. the tension is a constant value, the solution of the equation describing the adopted model is [Brinson 2015] [Bochnia 2017] [Bochnia 2016] in general form:

$$b_2\frac{d^2}{dt^2}\varepsilon(t)+b_1\frac{d}{dt}\varepsilon(t)+b_0\varepsilon(t)= =a_2\frac{d^2}{dt^2}\sigma(t)+a_1\frac{d}{dt}\sigma(t)+a_0\sigma(t) \quad (1)$$

With initial conditions: $\varepsilon_0(0)=0, \varepsilon_0'(0)=0$. Coefficiens of the eq. 1 are given as:

$$b_2 = E_0\mu_1\mu_2 \qquad a_2 = \mu_1\mu_2$$
$$b_1 = E_0(E_1\mu_2 + E_2\mu_1) \qquad a_1 = (E_1\mu_2 + E_2\mu_1 + E_0\mu_2 + E_0\mu_1)$$
$$b_0 = (E_0E_1E_2) \qquad a_0 = (E_0E_1 + E_0E_2 + E_1E_2)$$

For the case of simple creep loading $\sigma(t)=\sigma_0 H(t)$, where $H(t)$ is s the Heaviside function.

To solve eq. 1, Laplace transform was used. The general form of this transform for the second and first order derivatives can be written by the formulas:

$$\mathrm{L}\{\varepsilon''(t)\} = s^2\,\mathrm{L}[\varepsilon(t)] - s\varepsilon(0^+) - \varepsilon'(0^+) \quad (2)$$

$$\mathrm{L}\{\varepsilon'(t)\} = s\,\mathrm{L}[\varepsilon(t)] - \varepsilon(0^+) \quad (3)$$

Laplace transform for Heaviside and for delta Dirac function, written as:

$$\mathrm{L}\{\delta(t)\} = 1 \quad (4)$$

$$\mathrm{L}\{H(t)\} = \frac{1}{s} \quad (5)$$

$$\mathrm{L}\{\delta'(t)\} = s \quad (6)$$

Substituting relations 2-6 to eq. 1, we obtained

$$\mathrm{L}[\varepsilon(t)] = \varepsilon(s) = \frac{\sigma_0\left(a_2s + a_1 + a_0\frac{1}{s}\right)}{b_2s^2 + b_1s + b_0} = \frac{A}{b_2s} + \frac{B}{b_2\left(s+\frac{1}{\tau_1}\right)} + \frac{C}{b_2\left(s+\frac{1}{\tau_2}\right)} \quad (7)$$

where:

$t_1 = -\frac{\mu_1}{E_1}$, $t_2 = -\frac{\mu_2}{E_2}$ and $A = \sigma_0\left(\frac{1}{E_2}+\frac{1}{E_1}+\frac{1}{E_0}\right)$, $B = -\sigma_0\frac{1}{E_1}$ and $C = -\sigma_0\frac{1}{E_2}$.

After applying inverse Laplace transform of the relation obtained which describe the strain as a function of time.

$$\varepsilon(t) = \sigma_0\left(\frac{1}{E_0} + \left(\frac{1}{E_1}\left(1-e^{-\frac{t}{t_1}}\right) + \frac{1}{E_2}\left(1-e^{-\frac{t}{t_2}}\right)\right)\right) \quad (8)$$

or more suitable form:

$$\varepsilon(t) = \sigma_0\left(\frac{1}{E_0} + \sum_{i=1}^{n}\frac{1}{E_i}\left(1-e^{\frac{-t}{t_i}}\right)\right) \quad (9)$$

where: σ_0 – set tension, n – the number of basic models, i – the marking of the subsequent model number, t_i – delay time of the elastic Kevin i-th model, which amounts to:

$$t_i = \frac{\mu_i}{E_i} \quad (10)$$

where: μ_i – the coefficient of viscosity of the i-th model, E_i – the elastic modulus of the i-th model.
After transformations it takes the following form:

$$\varepsilon(t) = \varepsilon_0 + \varepsilon_1(1-e^{\frac{-t}{t_1}}) + \varepsilon_2(1-e^{\frac{-t}{t_2}}) \quad (11)$$

The equation (3) was applied to describe the creep of material that the samples were made of.

3 RESULTS

The curves 2 presented in Figure 3 were analyzed. The theoretical creep curves described with the equation (3) were adjusted to the experimental curves. The results thereof were shown in Figure 5a, b and c.

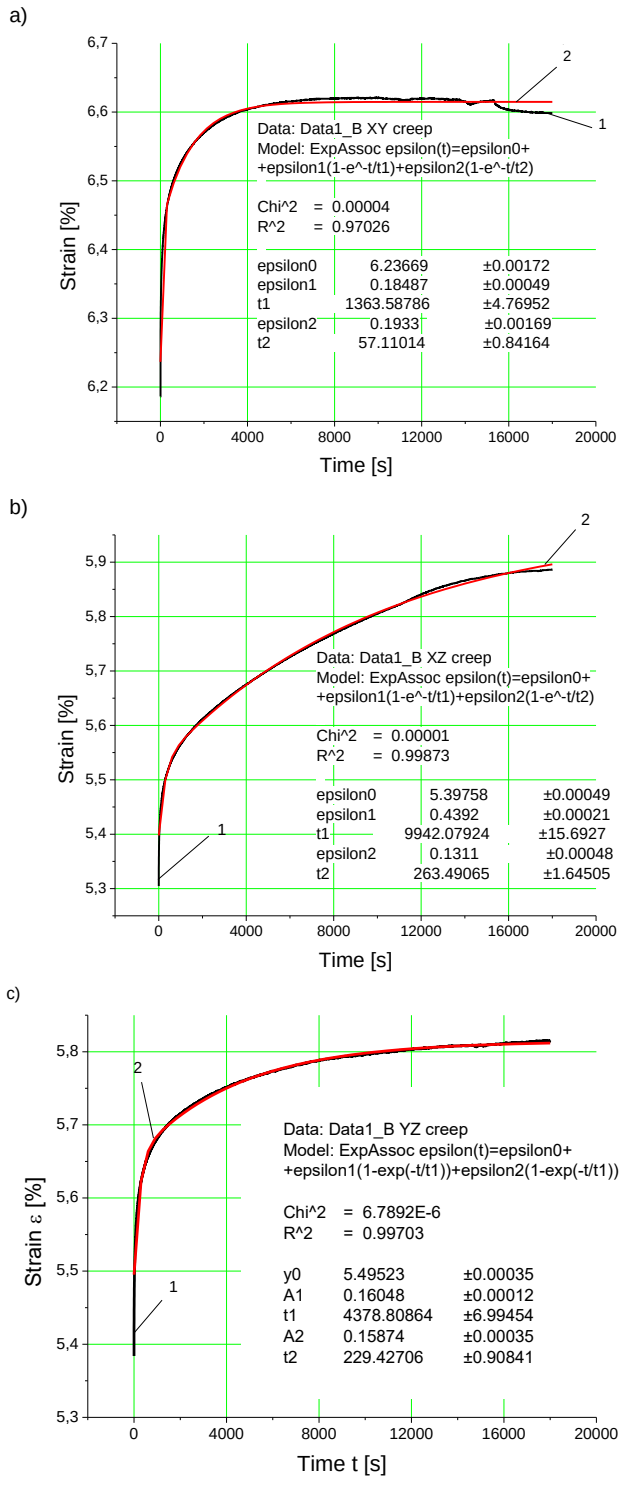

Figure 5: The results of the creep tests with the adjusted curves. 1 – experimental creep curves, 2 – creep curves approximated by the equation (3); a) the creep curves for the XY sample – Z print direction, b) the creep curves for the XZ sample– Y print direction, c) the creep curves for the YZ sample – X print direction.

The approximation with the use of the equation (3) was performed for the experimental curve, by specifying the parameter values ε_0, ε_1, ε_2, t_1, t_2 as well as the values or Chi^2 and R^2 tests. The values of those parameters were specified in Figure 5. A simple conclusion might be drawn on the basis of the qualitative assessment of Figure 5: the approximation curve was properly adjusted to the real-time (experimental) curve with the use of the equation (3). Based on the estimated values of ε_0, ε_1, ε_2, the values of the elastic modulus of the Kelvin-Voigt model used were calculated from equation (9). Table 1 contains the calculated values of the modules E_0, E_1 and E_2 as well as the delay times t_1 and t_2.

TEST SYMBOL	E_0 (MPa)	E_1 (MPa)	E_2 (MPa)	t_1 (s)	t_2 (s)
XZ	1,468	18,046	60,458	9942	262
YZ	1,442	49,389	49,931	9379	229
XY	1,271	42,873	41,004	1364	57

Table 1. Parameters obtained from creep curves for SLS technology, sample made of PA 2200.

On the basis of the obtained results the values of the elastic modulus E_0, E_1, E_2 as well as the viscosity coefficients μ_1 and μ_2 of the Kelvin-Voight model presented in Figure. 4 might be calculated.

Considering eqs. 9 or 11, for the case when t=0 the strain is:

$$\varepsilon(0)=\frac{\sigma_0}{E_0}=\varepsilon_0 \tag{12}$$

when t→∞ the strain takes the value:

$$\varepsilon\left(t_\infty\right)=\sigma_0\left(\frac{1}{E_0}+\frac{1}{E_1}+\frac{1}{E_2}\right) \tag{13}$$

Where $\frac{1}{E_{eq}}=\frac{1}{E_0}+\frac{1}{E_1}+\frac{1}{E_2}$ is equivalent elasticity module.

TEST SYMBOL	E_{eq} (MPa)	ε_0 (%)	ε_{eq} (%)
XZ	1,328	5,398	5,968
YZ	1,362	5,495	5,819
XY	1,199	6,237	6,611

Table 2. Values of the equivalent elasticity modules and strains for t=0 and t→∞ .

Based on equation (10) and data from Table 1, the values of coefficients μ_1 and μ_2 were calculated for individual samples. The results are summarized in table 3.

TEST SYMBOL	μ_1 (MPa·s)	μ_2 (MPa·s)
XZ	179400	15870
YZ	216300	11460

XY	58460	2342

Table 3. Values of coefficients μ_1 and μ_2 calculated for individual tests.

The approximation procedure carried out allowed the estimation of specific parameter values of the Kelvin-Voigt model used, which are summarized in Tables 1 and 3.

4 CONCLUSION

Estimation using the approximation of the parameters of the creep function (3) gives the full picture of the adjustment of the curves, and confirms usefulness of the adopted model of the ideal body model to the description of the real-time material. The description of the experimental creeping curve with the use of the ideal body model with the set approximation accuracy is of great importance due to the physical character of the obtained parameters. The anisotropy of the rheological material properties was detected with regard to the print direction. The experiment which was conducted broadens the knowledge about the properties of new materials manufactured with the use of the additive technologies, in this case – with the use of the SLS technology.

ACKNOWLEDGEMENT

This paper was prepared with the use of the equipment purchased from the project "Development of the research base of specialized laboratories of public universities in the Świętokrzyskie region". Priority 2: The infrastructure of the B+R zone, Measure 2.2. Support for common research infrastructure for scientific units under the Innovative Economy Operational Program (Pol. Program Operacyjny Innowacyjna Gospodarka), the project No. POIG 02.02.00-26-023/08-00.

REFERENCES

[Adamczak 2017] Adamczak, S., Zmarzly, P., Kozior, T. and Gogolewski, D. ANALYSIS OF THE DIMENSIONAL ACCURACY OF CASTING MODELS MANUFACTURED BY FUSED DEPOSITION MODELING TECHNOLOGY, In: Fuis, V. (Ed.), ENGINEERING MECHANICS 2017, ACAD SCI CZECH REPUBLIC, INST THERMOMECHANICS, pp. 66–69. 978-80-214-5497-2.

[Bass 2016] Bass, L., Meisel, N. A. and Williams, C. B. Exploring variability of orientation and aging effects in material properties of multi-material jetting parts. *RAPID PROTOTYPING JOURNAL*, 2016, Vol. 22, 5, SI, pp. 826–834. 1355-2546, DOI:10.1108/RPJ-11-2015-0169.

[Blasiak 2014] Blasiak, S., Takosoglu, J. E. and Laski, P. A. OPTIMIZING THE FLOW RATE IN A PNEUMATIC DIRECTIONAL CONTROL VALVE, In: Fuis, V. (Ed.), ENGINEERING MECHANICS 2014, ACAD SCI CZECH REPUBLIC, INST THERMOMECHANICS, pp. 96–99. 978-80-214-4871-1.

[Blasiak 2016] Blasiak, S. Time-fractional heat transfer equations in modeling of the non-contacting face seals. *INTERNATIONAL JOURNAL OF HEAT AND MASS TRANSFER*, 2016, Vol. 100, pp. 79–88. 0017-9310, DOI:10.1016/j.ijheatmasstransfer.2016.04.040.

[Bochnia 2016] Bochnia, J. and Blasiak, S. ANISOTROPHY OF MECHANICAL PROPERTIES OF A MATERIAL WHICH IS SHAPED INCREMENTALLY USING POLYJET TECHNOLOGY, In: Zolotarev, I., Radolf, V. (Eds.), ENGINEERING MECHANICS 2016, ACAD SCI CZECH REPUBLIC, INST THERMOMECHANICS, 74+. 978-80-87012-59-8.

[Bochnia 2017] Bochnia, J. RELAXATION OF MATERIALS OBTAINED USING POLYJET TECHNOLOGY, In: Fuis, V. (Ed.), ENGINEERING MECHANICS 2017, ACAD SCI CZECH REPUBLIC, INST THERMOMECHANICS, pp. 178–181. 978-80-214-5497-2.

[Brinson 2015] Brinson, Hal F; Brinson, L. Catherine. Polymer Engineering Science and Viscoelasticity, Boston, MA. doi.org/10.1007/978-1-4899-7485-3: Springer US, 2015. 978-1-4899-7484-6.

[Gibson 2010] Gibson, Ian; Rosen, David W; Stucker, Brent. Additive Manufacturing Technologies, Boston, MA. doi.org/10.1007/978-1-4419-1120-9: Springer US, 2010. 978-1-4419-1119-3.

[Kozior 2019] Kozior, T., Trabelsi, M., Mamun, A., Sabantina, L. and Ehrmann, A. Stabilization of Electrospun Nanofiber Mats Used for Filters by 3D Printing. *Polymers*, 2019, Vol. 11, 10, DOI:10.3390/polym11101618.

[Nowakowski 2017] Nowakowski, L., Miko, E. and Skrzyniarz, M. DESIGNATION OF THE MINIMUM THICKNESS OF MACHINED LAYER FOR THE MILLING PROCESS OF DURALUMIN PA6, In: Fuis, V. (Ed.), ENGINEERING MECHANICS 2017, ACAD SCI CZECH REPUBLIC, INST THERMOMECHANICS, pp. 722–725. 978-80-214-5497-2.

[Schmidt 2017] Schmidt, J., Janda, T., Sejnoha, M. and Valentin, J. EXPERIMENTAL DETERMINATION OF VISCO-ELASIC PROPERTIES OF LAMINATED GLASS INTERLAYER, In: Fuis, V. (Ed.), ENGINEERING MECHANICS 2017, ACAD SCI CZECH REPUBLIC, INST THERMOMECHANICS, pp. 850–853. 978-80-214-5497-2.

[Takosoglu 2014] Takosoglu, J. E., Laski, P. A. and Blasiak, S. INNOVATIVE MODULAR PNEUMATIC VALVE TERMINAL WITH SELF-DIAGNOSIS, CONTROL AND NETWORK COMMUNICATIONS, In: Fuis, V. (Ed.), ENGINEERING MECHANICS 2014, ACAD SCI CZECH REPUBLIC, INST THERMOMECHANICS, pp. 644–647. 978-80-214-4871-1.

[Vasquez 2014] Vasquez, G. M., Majewski, C. E., Haworth, B. and Hopkinson, N. A targeted material selection process for polymers in laser sintering. *Additive Manufacturing*, 2014, Vol. 1-4, pp. 127–138, DOI:10.1016/j.addma.2014.09.003.

[Verbelen 2017] Verbelen, L., Dadbakhsh, S., van den Eynde, M., Strobbe, D., Kruth, J.-P., Goderis, B. and van Puyvelde, P. Analysis of the material properties involved in laser sintering of thermoplastic polyurethane. *Additive Manufacturing*, 2017, Vol. 15, pp. 12–19, DOI:10.1016/j.addma.2017.03.001.

CONTACTS:

dr hab. inż. Jerzy Bochnia
Kielce University of Technology, Faculty of Mechatronics and Mechanical Engineering, Department of Mechanical Technology and Metrology, Al. Tysiaclecia Panstwa Polskiego 7, 25-314, Kielce, Poland
+48 41 34 24 756, jbochnia@tu.kielce.pl, www.tu.kiece.pl